

From Eye to Mind: brain2text Decoding Reveals the Neural Mechanisms of Visual Semantic Processing

Author Information

Affiliations

Feihan Feng¹⁻⁵ & Jingxin Nie^{1-5*}

¹Philosophy and Social Science Laboratory of Reading and Development in Children and Adolescents (South China Normal University), Ministry of Education Center for Studies of Psychological Application, South China Normal University; Guangzhou, 510631, China.

²Center for Studies of Psychological Application, South China Normal University; Guangzhou, 510631, China.

³Key Laboratory of Brain, Cognition and Education Sciences (South China Normal University), Ministry of Education.

⁴School of Psychology, South China Normal University; Guangzhou, 510631, China.

⁵Guangdong Key Laboratory of Mental Health and Cognitive Science, South China Normal University; Guangzhou, 510631, China.

Abstract

Deciphering the neural mechanisms that transform sensory experiences into meaningful semantic representations is a fundamental challenge in cognitive neuroscience. While neuroimaging has mapped a distributed semantic network, the format and neural code of semantic content remain

elusive, particularly for complex, naturalistic stimuli. Traditional brain decoding, focused on visual reconstruction, primarily captures low-level perceptual features, missing the deeper semantic essence guiding human cognition. Here, we introduce a paradigm shift by directly decoding fMRI signals into textual descriptions of viewed natural images. Our novel deep learning model, trained without visual input, achieves state-of-the-art semantic decoding performance, generating meaningful captions that capture the core semantic content of complex scenes. Neuroanatomical analysis reveals the critical role of higher-level visual regions, including MT+, ventral stream visual cortex, and inferior parietal cortex, in this semantic transformation. Category-specific decoding further demonstrates nuanced neural representations for semantic dimensions like animacy and motion. This text-based decoding approach provides a more direct and interpretable window into the brain's semantic encoding than visual reconstruction, offering a powerful new methodology for probing the neural basis of complex semantic processing, refining our understanding of the distributed semantic network, and potentially inspiring brain-inspired language models.

Introduction

Humans seamlessly navigate the world through semantic understanding, effortlessly transforming sensory experiences into meaningful concepts that underpin language, object recognition, and social interaction. Deciphering the neural mechanisms of this fundamental cognitive ability remains a central challenge in neuroscience. Functional neuroimaging has consistently implicated a distributed, left-lateralized semantic network, broadly organized into representation and control systems^{1,2}. Within this network, regions such as the middle temporal gyrus (MTG) and the anterior temporal lobe (ATL) are crucial for representing multimodal conceptual knowledge, while the inferior frontal gyrus (IFG) is thought to orchestrate semantic access and contextual adaptation^{3,4,5}. Despite substantial progress

in mapping this network, a critical question endures: how does the brain encode the rich and nuanced semantic information derived from complex, real-world experiences?

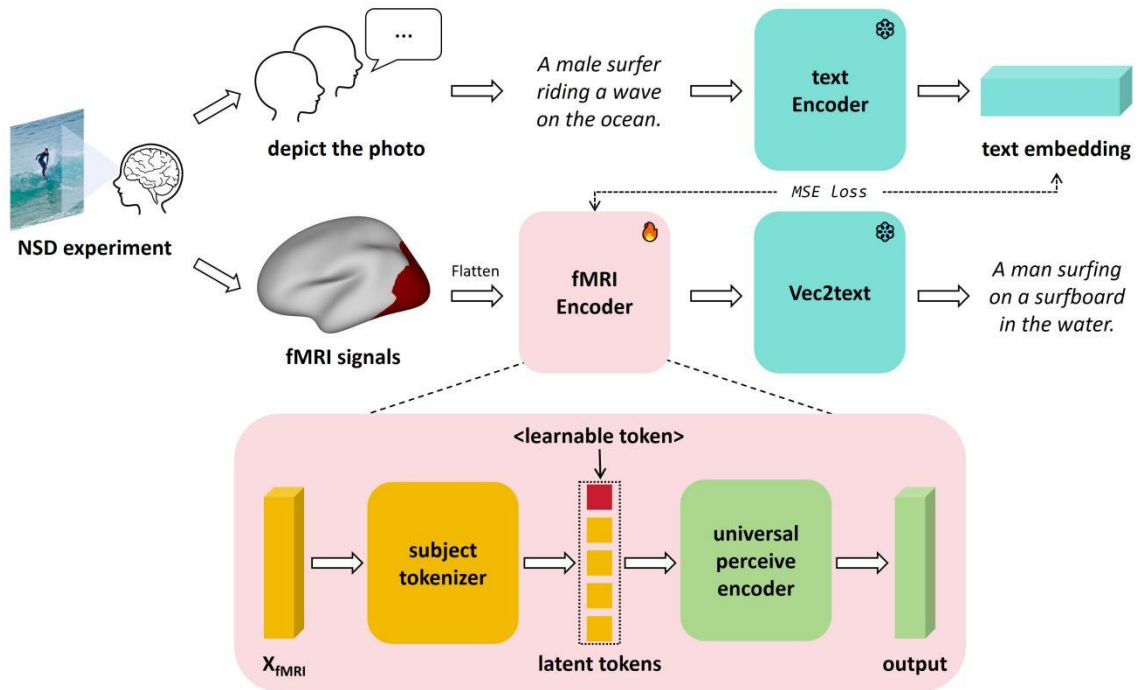
Early theories proposed that semantic categories are represented in spatially segregated brain regions^{6, 7, 8, 9}. However, the sheer breadth of human conceptual knowledge challenges this localized view. A more compelling alternative suggests that semantic representations emerge from distributed patterns of perceptual and motor features, embodying the principles of embodied cognition^{10, 11, 12, 13}. Computational models have begun to capture this distributed nature, often relying on linear approaches and simplified feature encoding^{14, 15, 16}. While informative, these methods may not fully capture the inherent non-linearities and hierarchical organization that characterize neural semantic processing. Moreover, many studies utilize linguistic stimuli, potentially lacking the ecological validity inherent in rich, natural visual scenes.

Vision, as our dominant sensory modality, provides an unparalleled source of semantic information. Natural images, in particular, offer complex, ecologically relevant stimuli that elicit robust neural responses, providing a powerful avenue for investigating semantic understanding¹⁷. Recent technological advances, combining large-scale fMRI datasets of natural image viewing, such as the Natural Scenes Dataset (NSD)¹⁸, with deep learning techniques, have opened exciting new possibilities for reconstructing perceptual experiences from brain activity. Initial efforts focused on reconstructing low-level visual features like edges and colors^{19, 20}. While generative models have since improved reconstruction fidelity^{21, 22, 23, 24}, a key limitation persists: these methods primarily capture visual appearance, often overlooking the deeper, abstract semantic content that is central to human cognition. Consequently, the critical neural transformation from visual input to meaningful semantic interpretation remains largely elusive.

To overcome these limitations, we introduce a novel approach that moves beyond pixel-level reconstruction by directly decoding fMRI signals into textual descriptions of viewed natural images. This strategy compels computational models to articulate the high-level semantic essence of visual scenes, encompassing objects, actions, relationships, and contextual information – thus mirroring the richness of human semantic understanding. By translating brain activity directly into language-based descriptions, we aim to tap into the neural processes underpinning abstract semantic representation, circumventing intermediate visual representations. We hypothesize that decoding to text provides a more direct and interpretable window into the brain’s semantic encoding mechanisms than traditional visual reconstruction paradigms.

To validate this hypothesis, we leverage the Natural Scenes Dataset (NSD) and developed a novel deep learning framework (Fig. 1) to predict semantic vector representations of human-generated image captions directly from fMRI signals. This framework incorporates subject-specific brain tokenization and a shared perceive encoder, followed by a Vec2Text decoder to generate comprehensive captions²⁵. This approach offers several advantages, providing direct access to high-level semantic content by bypassing low-level visual features, offering enhanced interpretability through naturally language-based descriptions of neural activity, and bridging the gap between perception and cognition by illuminating the neural transformations from visual input to abstract semantic understanding. Furthermore, by employing explainable AI techniques, such as SHAP values²⁶, we aim to dissect the contributions of specific regions of interest (ROIs), identify brain regions critical for visual semantic processing, and characterize activation patterns associated with distinct semantic categories.

Fig. 1: Overview of the research.



Results

Fig. 2: Samples of image captions.



A man surfing on a surfboard in the water.

A person in a wetsuit surfing on a turquoise wave.
A male surfer riding a wave on the ocean.
A young man with a surfboard at the ocean waters surfing
A surfer is riding the top of a wave.
a person standing on a surfboard riding a wave



A large airplane flying in the sky.

A lone airplane is flying high against a grey sky.
A large passenger jet flying through a gray sky.
A China Southern airliner flying on a cloudy day.
A airliner with Chinese writing imprinted on the side is in the air.
The large passenger plane is just taking off.



Two zebras are standing in a field of grass walking next to each other.

A couple of zebra walking across a grass covered field.
An adult and juvenile zebra standing in low grass in a field.
two zebra standing on a grassy field side by side
An adult and young zebra standing in a field of green grass.
A zebra and her baby are grazing in the field.



A person flying a kite in the sky on a green field.

A man flying a kite on top of a sandy field.
A man is standing in a field and flying a kite.
A person is flying a kite in the sky.
The man in in the field alone flying his kite.
A man is flying a kite on a bare area near some residential buildings, street lamps, and a car.



A man in a yellow shirt catching a Frisbee in the air.

A man outdoors jumping to catch a frisbee.
some people on a blanket and a frisbee player
A man jumps to catch a frisbee with two hands
A man is jumping in the air to catch a frisbee while people are sitting on a blanket
in the grass behind him.
A boy is jumping catching a Frisbee in the yard out on the grass



A fire hydrant with a yellow and red spray sits on the street next to a dirt road.

A fire hydrant on the corner of a neighborhood street
A fire hydrant on the corner of a street.
A yellow and green fire hydrant sitting on the side of a road.
The fire hydrant is green and yellow.
A fire hydrant sitting near a sign beside the street.

Images and corresponding image captions. Blue text indicates captions reconstructed from fMRI signals via the proposed model; black text shows corresponding human-provided ground truth captions.

Evaluation of the model's performance

This study introduces a paradigm shift in brain decoding, moving beyond visual reconstruction to directly access the semantic content of natural images as represented in fMRI signals. Fig. 2 showcases exemplar captions generated by our novel deep learning model directly from participant brain activity, alongside human-provided reference captions. Strikingly, even without pixel-level visual input, the model demonstrates a robust ability to capture the core semantic essence of complex scenes, evidenced by the meaningful, albeit not perfectly detailed or grammatically flawless, captions produced. This initial qualitative assessment underscores the fundamental capacity of our approach to tap into the neural code for semantic meaning.

To quantitatively evaluate model performance and optimize its architecture, we first conducted hyperparameter tuning using fMRI data from a representative participant (subj01) and assessed decoding accuracy using the CLIP score²⁷ (Supplementary Table 2). This analysis revealed that semantic information could be effectively decoded with a relatively parsimonious model architecture, while excessive parameterization led to overfitting and performance degradation. Based on these findings, we established an optimal model configuration with a latent channel dimension of 4 and a transformer depth of 4.

Table 1 Evaluation results

Method	BLEU1	BLUE2	BLEU3	BLEU4	METEOR	ROUGE	CIDEr	SPICE	CLIP-S	RefCLIP-S
Noise Ceiling	87.07	69.31	52.28	38.80	36.98	61.97	136.78	32.10	80.27	85.74
SDRecon	36.21	17.11	7.72	3.43	10.03	25.13	13.83	5.02	61.07	66.36
OneLLM	47.04	26.97	15.49	9.51	13.55	35.05	22.99	6.26	54.80	61.28
BrainCap	55.96	36.21	22.70	14.51	16.68	40.69	41.30	9.06	64.31	69.90
UMBRAE	57.84	38.43	25.41	17.17	18.70	42.14	53.87	12.27	66.10	72.33
Ours (Higher-level ROIs)	56.79	36.47	21.85	13.07	21.56	43.20	47.84	14.01	69.14	74.07
Ours (All ROIs)	54.94	35.28	21.06	12.41	20.61	41.83	42.02	13.03	67.90	72.56
Ours (Lower-level ROIs)	39.26	18.60	6.15	2.17	11.76	30.97	2.47	2.87	44.00	47.02

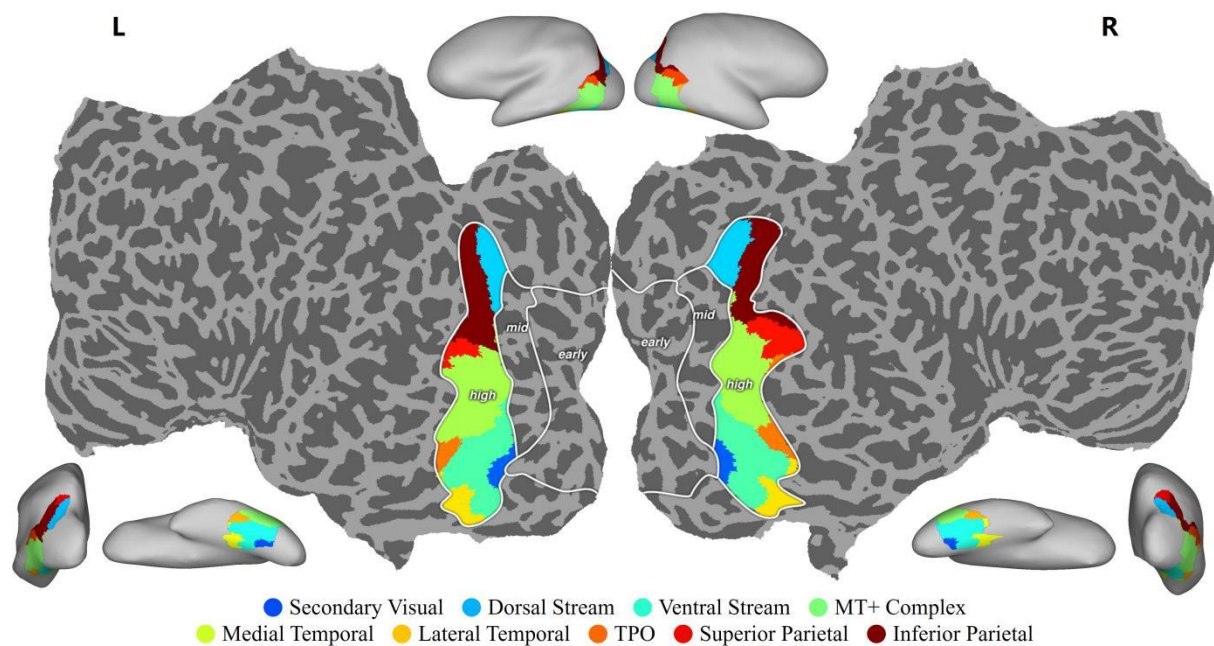
Evaluation results of our model and other method. ‘Higher-level ROIs’ refers to the model trained with brain regions of higher-level visual cortex. ‘ALL ROIs’ refers to the model trained with same input data as methods above. ‘Lower-level ROIs’ refers to the model trained with voxels except higher-level ROIs. ‘Noise Ceiling’ refers to the theoretical upper bound of model’s performance. The color red represents the best performance, orange indicates the second-best, and yellow denotes the third-best. Our model achieved not only the best performance on high-level metrics, such as CLIP scores, but also comparable performance on low-level metrics, such as BLEU scores.

We then benchmarked our text-decoding model against existing state-of-the-art brain captioning models^{22, 24, 28, 29}, all utilizing visual cortex voxel data from subj01. Notably, while prior models primarily rely on image embeddings as intermediate representations, our model achieves comparable performance without leveraging any visual information whatsoever (Table 1). This key distinction highlights the power of our direct text-decoding approach to access semantic representations directly from neural activity, rather than indirectly through visual proxies. Furthermore, we observed a critical neuroanatomical specificity: models trained on higher-level visual cortex ROIs, known to be involved in later stages of visual processing, significantly outperformed models using all visual cortex voxels

or those focused on early visual cortex ROIs. This finding, further substantiated by SHAP value analysis (Supplementary Fig. 1), directly implicates higher-level visual areas as holding a dominant role in encoding semantic content. Consistent with the notion that data quality is paramount in neuroimaging, evaluations across four participants revealed that enhanced fMRI data quality correlated with improved semantic reconstruction performance (Supplementary Table 1). Consequently, higher-level ROIs were established as the optimal input for subsequent in-depth analyses.

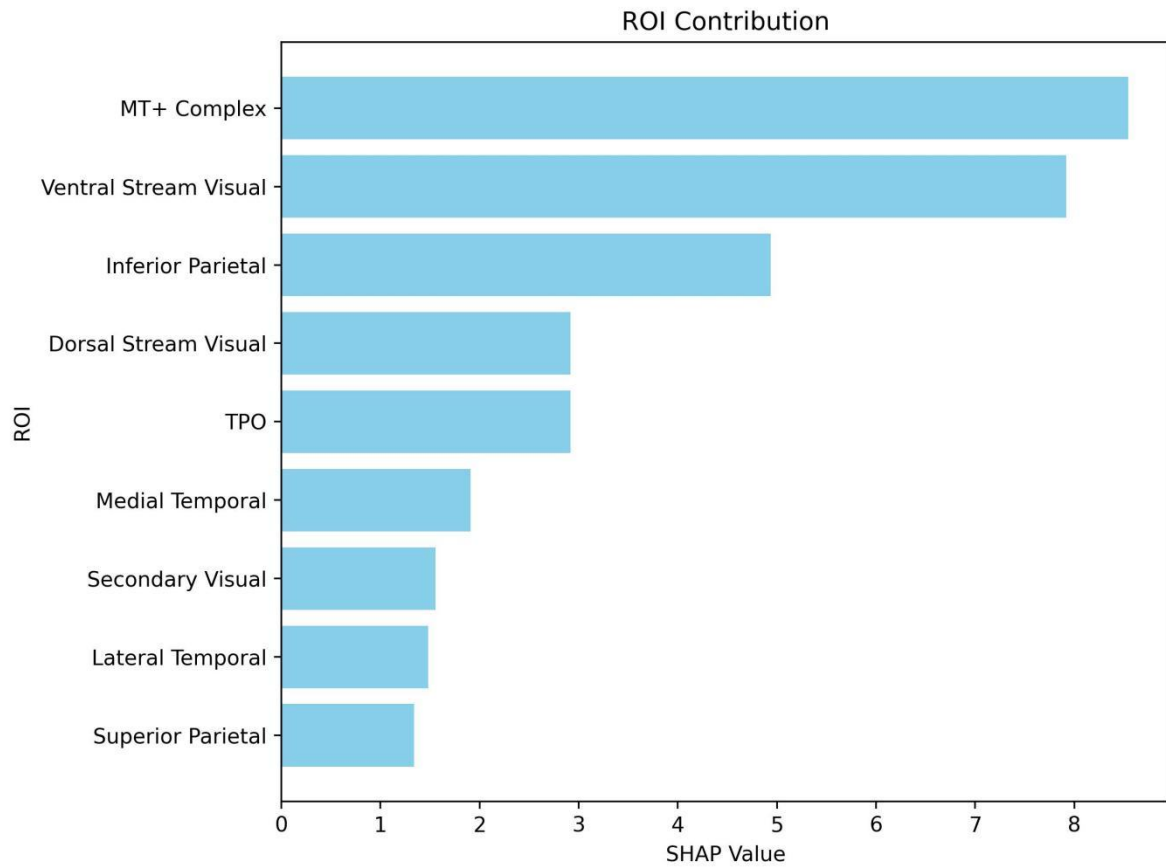
Interpreting the Neural Basis of Semantic Processing

Fig. 3: ROI's map.



This flattened cortex shows the parcellation of input voxels. The white contour delineates the "nsdgeneral" mask, representing visual cortex voxels conventionally used as model input in previous methods. The colored areas correspond to higher-level visual regions identified through the HCP_MMP atlas. ('early', early visual cortex ROI; 'mid', the intermediate ROIs; 'high', the higher-level ROIs; 'TPO', temporo-parieto-occipital junction)

Fig. 4: Contribution of higher-level ROIs.



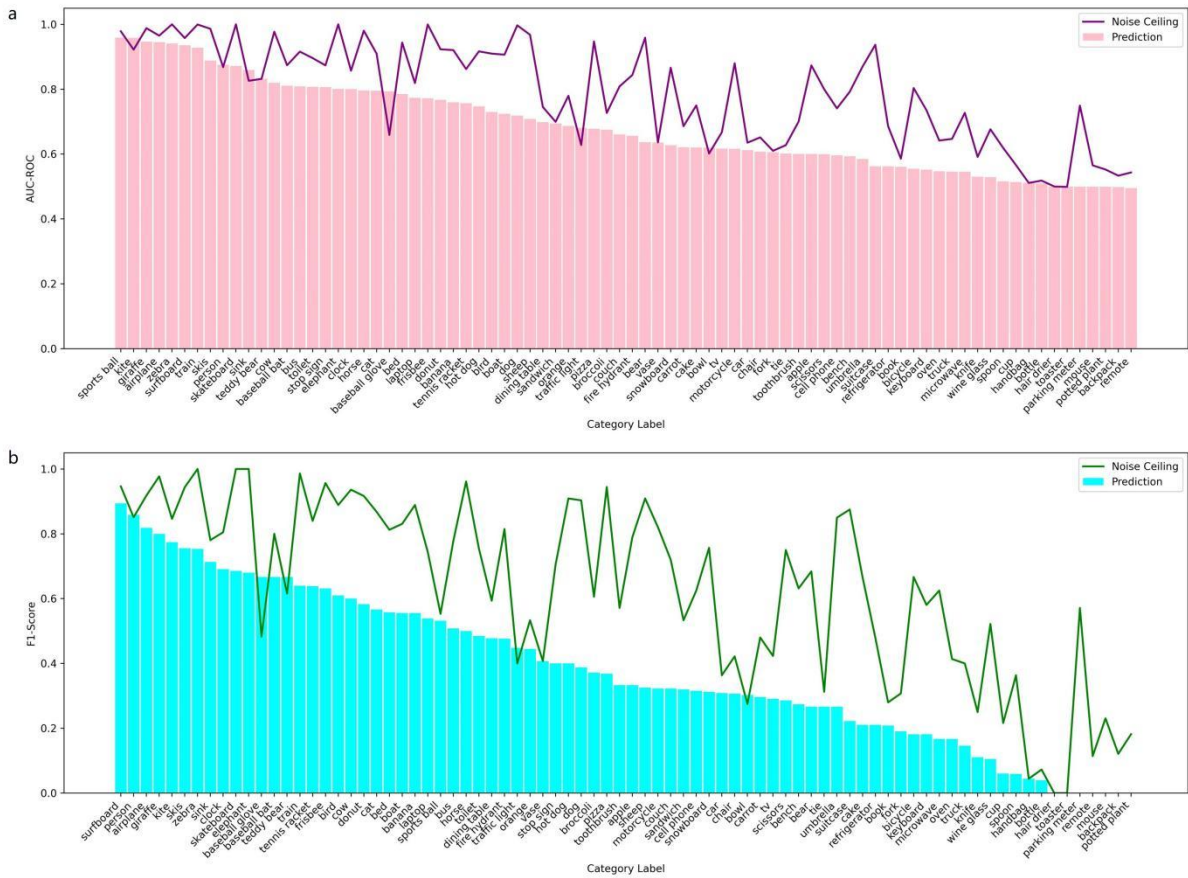
The contribution of distinct brain regions in higher-level visual cortex to visual semantic decoding performance using SHAP values.

To dissect the neural substrates of semantic processing, we leveraged SHAP values to quantify the contribution of different brain regions to our text-decoding model's performance. Fig. 4 presents the contribution of different brain regions to the CLIP scores in our model. The MT+ complex, ventral stream visual and inferior parietal regions make substantial contributions to the model's performance, suggesting that these regions represent majority of semantic information in visual semantic processing. In contrast, the dorsal stream visual and TPO regions exhibit relatively lower contributions. Other regions may play a role unrelated to representing semantic information in semantic processing or may not be involved in semantic processing, instead reflecting the model's attribution tendencies across

input features. As shown in Supplementary Fig. 1, although regions outside the higher-level ROIs contribute positively to the model’s performance, their removal still improves the model’s performance.

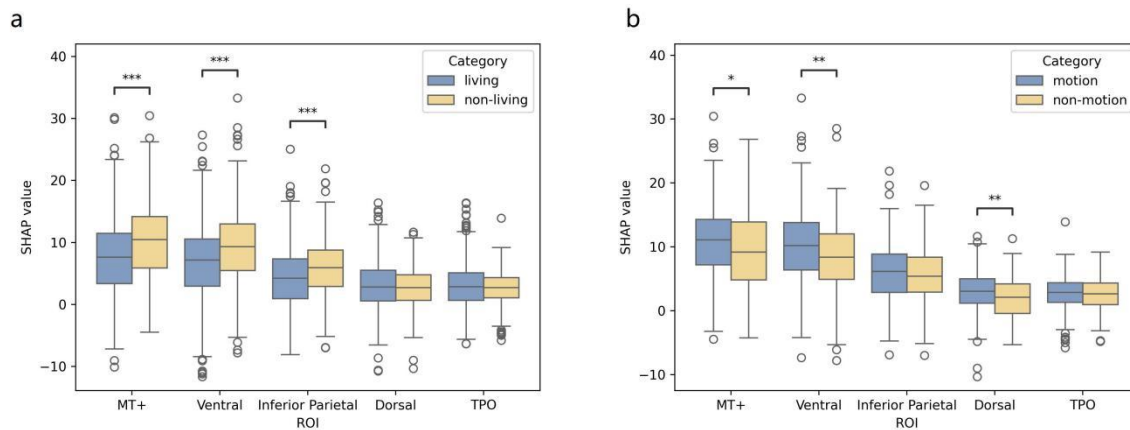
Category-specific semantic decoding

Fig. 5: Semantic label classification.



Performance in category-specific classification based on reconstructed text, reflecting the model’s ability to decode distinct semantic content that categorized according to 80 labels of ground truth images in the COCO dataset. a, Evaluation based on AUC-ROC. b, Evaluation based on F1 score.

Fig. 6: Semantic differences on ROIs.



SHAP values reveal distinct contributions of brain regions to visual semantic processing (higher SHAP values indicating greater involvement in the corresponding semantic categories). a, Difference in contribution across five ROIs between images with living (human and animals) and those without living content. b, Difference in contribution across five ROIs within non-living images, revealing the difference of images with and without motion-related objects and scenes. Statistical significance was assessed using permutation tests ($n=10,000$). (, $p<0.05$; **, $p<0.01$; ***, $p<0.001$)*

To investigate the neural encoding of diverse semantic categories, we categorized images and analyzed model performance across 80 distinct semantic categories using a Large Language Model (Llama3-8B). Fig. 5 presents the classification results evaluated with AUC-ROC and F1 score, and noise ceiling was calculated to indicate the theoretical upper bound of model's performance. Our model effectively decodes semantic information containing the category "person", which aligns with the functional specialization of brain regions (e.g., FFA, EBA) in mediating selective recognition of human features^{7, 30}. It also demonstrates reasonable performance in reconstructing semantic information for motion-related concepts (e.g., "surfboard"), animals (e.g., "giraffe", "zebra"), and scenes involving "airplane" and "train". However, as expected, decoding accuracy varied across categories, with certain object categories (e.g., "backpack," "suitcase") proving more challenging.

This variability likely reflects differences in neural representation strength, perceptual saliency, or the complexity of semantic features associated with different categories.

To analyze the relationship between semantic categories and different brain regions, we classified reconstructed text into "living" (animals/humans) and "non-living" categories based on ground truth semantic labels, with non-living items subdivided into two groups defined by the presence of motion-related objects and scenes (e.g., "surfboard"). Permutation tests were applied to reveal differences in the SHAP values across five ROIs that contributed markedly to decoding. Quantitative analysis revealed significantly lower CLIP scores for the "living" category ($M = 68.5$, $SD = 12.4$) compared to the "non-living" category ($M = 70.3$, $SD = 11.3$) in overall decoding performance (permutation test, $\Delta = -1.81$, $p = 0.04$). The "living" category also exhibited significantly lower SHAP values in the MT+ complex, ventral stream visual and inferior parietal regions (Fig. 6a). The motion-related items are associated with significantly higher SHAP values in the MT+ complex, ventral stream visual and dorsal stream visual regions, however there are no significant differences in CLIP scores compared to "non-motion" items (Fig. 6b).

Discussion

In this study, we propose a model that decodes semantic information of natural images from fMRI signals without using any visual information of ground truth images. It demonstrates that only a small number of parameters (about 124M parameters for a single subject and about 156M parameters for all four subjects) are needed to decode semantic content from brain signals and achieve state-of-the-art performance. Further analysis based on model not only provides further support for current neuroscience findings on visual semantic processing, but also reveals the neural mechanisms of brain's semantic representation engaged by distinct complex visual semantic contents.

Our ROI-based analysis provides compelling evidence for the distributed nature of semantic representation and the critical roles of specific brain regions within the established semantic network¹⁶. Consistent with prior research^{31, 32, 33, 34}, we found that the MT+ complex, ventral stream visual cortex, and inferior parietal regions are key contributors to successful semantic decoding. These regions, functionally characterized by their involvement in motion perception and object recognition (MT+ complex), static object feature processing and semantic concept formation (ventral stream), and higher-level cognitive functions including attention and semantic processing (inferior parietal cortex), demonstrably act synergistically in representing and integrating semantic information from complex visual scenes. The SHAP value analysis robustly reinforces this view, highlighting the disproportionate contribution of these higher-level ROIs to model performance and emphasizing their central role in visual semantic processing, particularly for complex, ecologically valid stimuli.

Further dissecting model performance across semantic categories revealed nuanced aspects of neural representation. While our model effectively decoded the presence of semantic information related to "person" and "motion," reflecting the functional specialization of brain areas for these domains^{7, 30}, the accuracy of detailed semantic reconstruction did not significantly surpass other categories. This nuanced result may reflect the inherent complexity of motion-related semantic representations, potentially encompassing richer spatio-temporal dynamics and engaging broader neural networks beyond the visual cortex, even when presented in static images³⁵. Furthermore, the high decoding accuracy for categories like "zebra" and "airplane" may stem from their distinctive visual features (e.g., texture, size) that are readily encoded and lead to unique and easily decodable neural patterns. Conversely, the challenges in decoding categories like "backpack" and "suitcase," often contextually embedded within scenes or associated with persons, and small objects like "spoon" and "cup," suggest

potential attention selection biases in naturalistic visual processing. Intriguingly, analysis of noise ceiling even within human-provided captions indicated inherent incompleteness in semantic retrieval for some categories, further reflecting the complexities of human attention and semantic processing of rich visual scenes in the absence of explicit task demands.

Compared to previous approaches employing image captioning models or multimodal LLMs, our text-based decoding method demonstrates distinct advantages. Lower-level textual metrics (e.g., BLEU-k, ROUGE, CIDEr), focusing on lexical and syntactic similarity, yielded lower scores. However, higher-level semantic metrics (SPICE, CLIP-based scores), capturing semantic and contextual fidelity, revealed superior performance. This dissociation underscores a critical point: while token-based text generation models excel at lexical and syntactic tasks, sentence embedding-based approaches, like ours, are better suited for capturing holistic semantic information and contextual coherence from brain signals. Despite minor deviations in syntax and wording compared to reference captions, our method demonstrably recovers more accurate and meaningful semantic information, especially when dealing with the complex visual and conceptual demands of natural images. This highlights the power of text-based decoding for probing higher-level semantic processing in the brain.

Our findings further illuminate the neural instantiation of embodied and distributed semantic theories¹². The observation that "living" categories showed reduced decoding performance and lower SHAP values across key ROIs, compared to "non-living" categories, suggests that recognition of living things may rely on the more synergistic and distributed activation of a broader neural network³⁶. In contrast, motion-related items were associated with enhanced contributions from MT+ complex and dorsal stream visual regions, directly implicating these areas, traditionally linked to motion

perception and spatial processing, in representing objects with motion-related features or functions³⁷. Notably, we also found that ventral stream visual regions, typically associated with static object recognition, encoded significant information about motion-related objects. This suggests a more distributed and integrated network for encoding motion information than traditionally appreciated, involving both dorsal and ventral visual pathways. The temporoparietal occipital (TPO) junction, a region implicated in higher-level cognition³⁸, showed a consistent contribution across semantic categories, potentially reflecting its role in more abstract semantic functions, non-modal semantic representation, or higher-level semantic integration, rather than category-specific semantic processing. To further refine our understanding of semantic processing within the brain, future research should expand the scope of neuroimaging data beyond traditional visual cortices. Incorporating voxels from a broader network of brain regions known to contribute to advanced cognitive functions, particularly those implicated in semantic integration and higher-order association, is crucial. Such an approach would illuminate how distributed neural networks collaboratively encode and integrate high-level semantic content derived from complex visual scenes. Furthermore, future modeling efforts should prioritize theory-driven feature extraction, informed by established principles of embodied cognition and other relevant neuroscientific frameworks. This integration of psychological and neuroscientific insights promises to not only enhance the interpretability of brain decoding results but also to uncover more ecologically valid neural representations of semantic information.

A critical component of our approach is the semantic embedding vector, which serves as the bridge between raw brain signals and high-level semantic interpretation. Given its central role in our model's performance, future work should aggressively investigate alternative LLM architectures and embedding strategies, including exploring transformer-based models optimized for nuanced semantic

capture and contextualized embeddings to enrich meaning representation. Critically, this line of inquiry offers the exciting potential to move beyond simply using LLMs for brain decoding, towards developing truly brain-inspired language models.

In conclusion, this study presents a significant advancement in brain decoding by demonstrating the feasibility of directly reconstructing semantic content, in the form of textual descriptions, from fMRI signals. Our findings not only validate and refine current neuroscientific understanding of visual semantic processing but also introduce a powerful new methodology for investigating the neural basis of complex human cognition.

Methods

Dataset

We used the Natural Scenes Dataset (NSD) for our research. Briefly, NSD provides a large scale of high quality fMRI data acquired from a 7-Tesla fMRI scanner across 30-40 sessions, where each subject viewed 10,000 images from the COCO dataset³⁹ with each image repeated three times. Each image has five captions describing the content of the image and multiple labels of 80 categories. Here we used the data from four of all eight subjects (subj01, subj02, subj05, subj07). Each subject viewed 9,000 unique images (27,000 trials) and 1,000 shared images (3,000 trials). All 27,000 unique image trials were used as training data. For the test data, we averaged the three trials of each shared image, resulting in a test set of 1,000 images, which are consistent across all four subjects. As previous studies of decoding, we extracted the voxels from the "nsdgeneral", which indicates the occipital regions that generally responsive in the NSD experiment, along with other ROIs belonging to the selected voxels. These voxels would be flattened into 1D vectors and served as model input.

Model Architecture

Our model consists of two parts: an encoder that transforms fMRI signals into text embeddings, and a decoder that reconstructs brain captions from the resulting latent vectors. The encoder architecture, adapted from a previously established method²⁹, has demonstrated the ability to predict image embeddings from fMRI signals and perform downstream tasks such as image captioning, grounding, and visual decoding through the utilization of multimodal Large Language Models (LLMs). Additionally, the architecture is designed to train jointly across subject, which improves performance and enhances generalization. The encoding model comprises two main components: a subject-specific tokenizer that projects fMRI signals into a sequence of brain tokens, incorporating a learnable token that is independent of the inputs; and a universal lightweight transformer architecture that uses cross-attention mechanism to project the brain tokens into a latent bottleneck, extracting common knowledge across different subjects and generating predicted vectors. Subsequently, a convolution layer with the kernel size of 1×1 is added to aggregate information across channels. The encoder eventually outputs a 1536-dimensional vector, which is then fed into a text decoder called Vec2Text, to reconstruct a textual description corresponding to the image viewed by participant.

Our model incorporates two key hyperparameters: the number of latent channels of the subject-specific tokenizer and the depth of the universal transformer. In most hyperparameter configurations the model achieved performance close to the training limit, which exhibits overfitting. Thus, we set the number of latent channels to 4 and the depth of transformer to 4 to balance model's performance and training efficiency while minimizing complexity (Supplementary Table 2).

Vec2Text decoder

Vec2Text²⁵ is multi-step method that iteratively corrects and re-embeds text based on a fixed point in latent space. This model was trained to invert text embeddings from embedding models, and it

indicated a sort of equivalence between raw text and its embeddings, which enabled direct decoding of raw text from the text embeddings. Meanwhile, due to the semantic properties of the text embeddings, similar texts exhibit consistent vector directions, allowing the inversion model to preserve the original semantics, even when averaging these embeddings. Combining the approach with our model, we encoded the image captions into vectors using the text-embeddings-ada-002 model as ground truth, and predicted text embeddings from fMRI signals to reconstruct the semantic contents of visual stimuli in the experiment, generating description sentences for images without the need to relying on any visual information of ground truth images.

Training Strategy

Our model was trained on a single 4090 GPU for 200 epochs with a batch size of 256 per subject, totaling 1024 samples across four subjects. Prior to formal training, we conducted preliminary experiments using only data from subj01, selecting the best hyperparameters. We used AdamW⁴⁰ as the optimizer with $\beta_1 = 0.9$, $\beta_2 = 0.95$, and weight decay of 0.01. For the learning rate scheduler, we used one-cycle⁴¹ with an initial and max learning rate of 1e-3, we stopped training and saved the best model checkpoint after overfitting occurred. Mean Squared Error (MSE) was used as the loss function. To enhance model generalization, one of the five captions for each ground truth image was randomly selected as reference in training stage.

Semantic Categorization

The images used in the NSD experiment, sourced from the COCO dataset, have multiple semantic labels that span 80 categories. In our study, we employed the Large Language Model (Llama3-8B) to categorize the reconstructed text generated by our model. The LLMs have demonstrated performance comparable to or exceeding that of humans on cognitive tasks, including but not limited to text

categorization and image-based tasks⁴². We set the prompt as: "Is [category] included in the content of this sentence? Answer with only yes or no: ", followed by the image semantics reconstructed from brain signals. This process determined whether each reconstructed text could be assigned to any of 80 semantic categories. In addition, images containing labels for person or animals are categorized into a "living" group, while other images are assigned to the "non-living" group. The "non-living" group is further subdivided based on the presence of motion-related objects and scenes (e.g., "surfboard", "bicycle").

ROI Selection

Here we used the stream mask based on the Wang's anatomical atlas of visual topographic⁴³ in the dataset to identify three broad ROIs belonging to the selected voxels: the early visual cortex ROI, the intermediate ROIs and the higher-level ROIs. To analyze the function of different regions during semantic processing, we used the SHAP values to calculate the contribution of different ROIs in the model using higher-level ROIs as input. And we applied the HCP_MMP atlas⁴⁴ to identified about 40 regions from the higher-level ROIs, which would be categorized into nine groups based on previous research after excluding regions with insufficient voxels⁴⁵, including the secondary visual cortex region, ventral stream visual region, dorsal stream visual region, MT+ complex region, medial temporal region, lateral temporal region, TPO (temporo-parieto-occipital junction) region, superior parietal region and inferior parietal region. Permutation tests were employed to evaluate the significance of semantic differences across ROIs, with the number of permutations set to 10,000.

Evaluation Metrics

For the evaluation of our model's performance, we selected five widely used Natural Language Processing metrics: BLEU-k⁴⁶, METEOR⁴⁷, ROUGE⁴⁸, CIDEr⁴⁹, SPICE⁵⁰, to assess the similarity

between ground truth text and generated text. In addition, two CLIP-based scores named CLIP-S and RefCLIP-S²⁷ were applied to evaluate the alignment between ground truth images and generated text, as well as between ground truth and generated text. For ROI analysis, we grouped the input voxels into larger brain regions for analysis given the number and function of brain voxels. We used SHAP values to quantify the average marginal contribution of each feature across all possible subsets, providing an unbiased estimate of feature importance. And CLIP-S was employed as the evaluation metric for the SHAP value analysis, assessing the contribution of each ROI to the decoding performance. Since all ground truth captions for each image were utilized during training phase, the text reconstructed from the average of their embeddings were evaluated using the aforementioned metrics and designated as the noise ceiling, indicating the theoretical upper bound of the model's performance.

Data Availability

The data used in our study were obtained from the Natural Scenes Dataset (NSD), which is publicly available for download at: <http://naturalscenesdataset.org>. (Ref. ¹⁸)

Code Availability

Our code is publicly available on GitHub (<https://github.com/AllenFung/brain2text>).

References

1. Binder JR, Desai RH, Graves WW, Conant LL. Where is the semantic system? A critical review and meta-analysis of 120 functional neuroimaging studies. *Cerebral cortex* **19**, 2767-2796 (2009).
2. Ralph MAL, Jefferies E, Patterson K, Rogers TT. The neural and computational bases of semantic cognition. *Nature reviews neuroscience* **18**, 42-55 (2017).
3. Lau EF, Phillips C, Poeppel D. A cortical network for semantics:(de) constructing the N400. *Nature reviews neuroscience* **9**, 920-933 (2008).

4. Patterson K, Nestor PJ, Rogers TT. Where do you know what you know? The representation of semantic knowledge in the human brain. *Nature reviews neuroscience* **8**, 976-987 (2007).
5. Davey J, *et al.* Shared neural processes support semantic control and action understanding. *Brain and language* **142**, 24-35 (2015).
6. Frisby SL, Halai AD, Cox CR, Ralph MAL, Rogers TT. Decoding semantic representations in mind and brain. *Trends in cognitive sciences* **27**, 258-281 (2023).
7. Kanwisher N, McDermott J, Chun MM. The Fusiform Face Area: A Module in Human Extrastriate Cortex Specialized for Face Perception. *The Journal of Neuroscience* **17**, 4302-4311 (1997).
8. Epstein R, Kanwisher N. A cortical representation of the local visual environment. *Nature* **392**, 598-601 (1998).
9. Caramazza A, Shelton JR. Domain-specific knowledge systems in the brain: The animate-inanimate distinction. *Journal of cognitive neuroscience* **10**, 1-34 (1998).
10. Aziz-Zadeh L, Wilson SM, Rizzolatti G, Iacoboni M. Congruent embodied representations for visually presented actions and linguistic phrases describing actions. *Current biology* **16**, 1818-1823 (2006).
11. Tyler LK, *et al.* Objects and categories: feature statistics and object processing in the ventral stream. *Journal of cognitive neuroscience* **25**, 1723-1735 (2013).
12. Fernandino L, *et al.* Concept representation reflects multimodal abstraction: A framework for embodied semantics. *Cerebral cortex* **26**, 2018-2034 (2016).
13. Liuzzi AG, Aglinskas A, Fairhall SL. General and feature-based semantic representations in the semantic network. *Scientific Reports* **10**, 8931 (2020).
14. Mitchell TM, *et al.* Predicting human brain activity associated with the meanings of nouns. *science* **320**, 1191-1195 (2008).
15. Huth AG, Nishimoto S, Vu AT, Gallant JL. A continuous semantic space describes the representation of thousands of object and action categories across the human brain. *Neuron* **76**, 1210-1224 (2012).
16. Huth AG, De Heer WA, Griffiths TL, Theunissen FE, Gallant JL. Natural speech reveals the semantic maps that tile human cerebral cortex. *Nature* **532**, 453-458 (2016).
17. Hasson U, Malach R, Heeger DJ. Reliability of cortical activity during natural stimulation. *Trends in cognitive sciences* **14**, 40-48 (2010).

18. Allen EJ, *et al.* A massive 7T fMRI dataset to bridge cognitive neuroscience and artificial intelligence. *Nature neuroscience* **25**, 116-126 (2022).
19. Shen G, Dwivedi K, Majima K, Horikawa T, Kamitani Y. End-to-end deep image reconstruction from human brain activity. *Frontiers in computational neuroscience* **13**, 432276 (2019).
20. Shen G, Horikawa T, Majima K, Kamitani Y. Deep image reconstruction from human brain activity. *PLoS computational biology* **15**, e1006633 (2019).
21. Lin S, Sprague T, Singh AK. Mind reader: Reconstructing complex images from brain activities. *Advances in Neural Information Processing Systems* **35**, 29624-29636 (2022).
22. Takagi Y, Nishimoto S. High-resolution image reconstruction with latent diffusion models from human brain activity. In: *Proceedings of the IEEE/CVF Conference on Computer Vision and Pattern Recognition* (2023).
23. Chen Z, Qing J, Xiang T, Yue WL, Zhou JH. Seeing beyond the brain: Conditional diffusion model with sparse masked modeling for vision decoding. In: *Proceedings of the IEEE/CVF Conference on Computer Vision and Pattern Recognition* (2023).
24. Ferrante M, Ozcelik F, Boccato T, VanRullen R, Toschi N. Brain Captioning: Decoding human brain activity into images and text. *arXiv preprint arXiv:230511560*, (2023).
25. Morris JX, Kuleshov V, Shmatikov V, Rush AM. Text embeddings reveal (almost) as much as text. *arXiv preprint arXiv:231006816*, (2023).
26. Lundberg S. A unified approach to interpreting model predictions. *arXiv preprint arXiv:170507874*, (2017).
27. Hessel J, Holtzman A, Forbes M, Bras RL, Choi Y. Clipscore: A reference-free evaluation metric for image captioning. *arXiv preprint arXiv:210408718*, (2021).
28. Han J, *et al.* Onellm: One framework to align all modalities with language. In: *Proceedings of the IEEE/CVF Conference on Computer Vision and Pattern Recognition* (2024).
29. Xia W, de Charette R, Öztireli C, Xue J-H. UMBRAE: Unified Multimodal Decoding of Brain Signals. *arXiv preprint arXiv:240407202*, (2024).
30. Downing PE, Jiang Y, Shuman M, Kanwisher N. A cortical area selective for visual processing of the human body. *Science* **293**, 2470-2473 (2001).
31. Maus GW, Fischer J, Whitney D. Motion-dependent representation of space in area MT+. *Neuron* **78**, 554-562 (2013).

32. Kourtzi Z, Bühlhoff HH, Erb M, Grodd W. Object-selective responses in the human motion area MT/MST. *Nature neuroscience* **5**, 17-18 (2002).
33. Seghier ML. The angular gyrus: multiple functions and multiple subdivisions. *The Neuroscientist* **19**, 43-61 (2013).
34. Chou T-L, Chen C-W, Wu M-Y, Booth JR. The role of inferior frontal gyrus and inferior parietal lobule in semantic processing of Chinese characters. *Experimental brain research* **198**, 465-475 (2009).
35. Proverbio AM, Riva F, Zani A. Observation of static pictures of dynamic actions enhances the activity of movement-related brain areas. *PLoS One* **4**, e5389 (2009).
36. Zannino GD, et al. Visual and semantic processing of living things and artifacts: an fMRI study. *Journal of cognitive neuroscience* **22**, 554-570 (2010).
37. Almeida J, Mahon BZ, Caramazza A. The role of the dorsal visual processing stream in tool identification. *Psychological science* **21**, 772-778 (2010).
38. De Benedictis A, et al. Anatomico-functional study of the temporo-parieto-occipital region: dissection, tractographic and brain mapping evidence from a neurosurgical perspective. *Journal of anatomy* **225**, 132-151 (2014).
39. Lin T-Y, et al. Microsoft coco: Common objects in context. In: *Computer Vision—ECCV 2014: 13th European Conference, Zurich, Switzerland, September 6-12, 2014, Proceedings, Part V 13*. Springer (2014).
40. Loshchilov I. Decoupled weight decay regularization. *arXiv preprint arXiv:1711.05101*, (2017).
41. Smith LN, Topin N. Super-convergence: Very fast training of neural networks using large learning rates. In: *Artificial intelligence and machine learning for multi-domain operations applications*. SPIE (2019).
42. Binz M, Schulz E. Using cognitive psychology to understand GPT-3. *Proceedings of the National Academy of Sciences* **120**, e2218523120 (2023).
43. Wang L, Mruczek RE, Arcaro MJ, Kastner S. Probabilistic maps of visual topography in human cortex. *Cerebral cortex* **25**, 3911-3931 (2015).
44. Glasser MF, et al. A multi-modal parcellation of human cerebral cortex. *Nature* **536**, 171-178 (2016).
45. Huang C-C, Rolls ET, Feng J, Lin C-P. An extended Human Connectome Project multimodal parcellation atlas of the human cortex and subcortical areas. *Brain Structure and Function* **227**, 763-778 (2022).

46. Papineni K, Roukos S, Ward T, Zhu W-J. Bleu: a method for automatic evaluation of machine translation. In: *Proceedings of the 40th annual meeting of the Association for Computational Linguistics* (2002).
47. Banerjee S, Lavie A. METEOR: An automatic metric for MT evaluation with improved correlation with human judgments. In: *Proceedings of the acl workshop on intrinsic and extrinsic evaluation measures for machine translation and/or summarization* (2005).
48. Lin C-Y. Rouge: A package for automatic evaluation of summaries. In: *Text summarization branches out* (2004).
49. Vedantam R, Lawrence Zitnick C, Parikh D. Cider: Consensus-based image description evaluation. In: *Proceedings of the IEEE conference on computer vision and pattern recognition* (2015).
50. Anderson P, Fernando B, Johnson M, Gould S. Spice: Semantic propositional image caption evaluation. In: *Computer Vision—ECCV 2016: 14th European Conference, Amsterdam, The Netherlands, October 11–14, 2016, Proceedings, Part V 14*. Springer (2016).

Acknowledgements

This work was supported by the Research Center for Brain Cognition and Human Development, Guangdong, China (No. 2024B0303390003); the Striving for the First-Class, Improving Weak Links and Highlighting Features (SIH) Key Discipline for Psychology in South China Normal University; Key-Area Research and Development Program of Guangdong Province (2019B030335001).

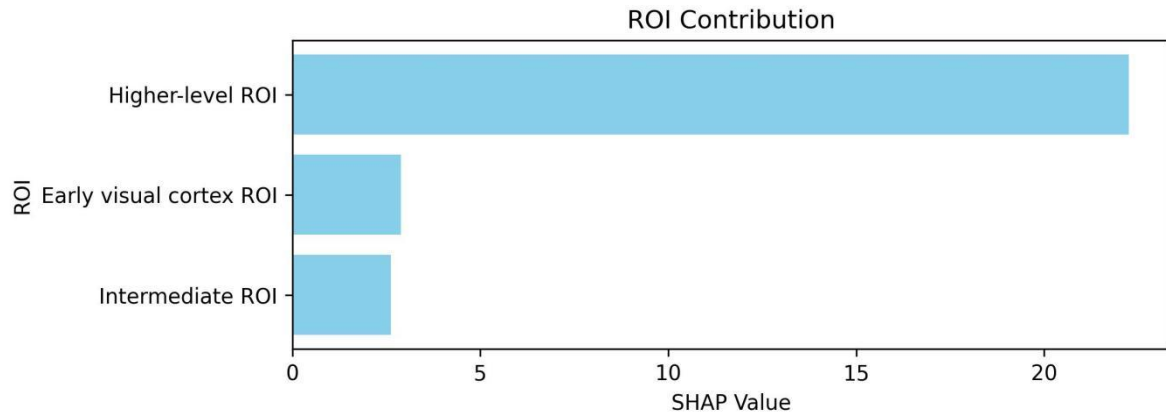
Ethics declarations

Competing interests

The authors declare no competing interests.

Supplementary Information

Fig. 1: Contribution of different functional areas of visual cortex.



The contribution of the three broad ROIs from the visual cortex of subj01, which align with the model input of previous studies, to the semantic decoding performance.

Table 1 Evaluation results of different participants

Subject ID	BLEU1	BLUE2	BLEU3	BLEU4	METEOR	ROUGE	CIDEr	SPICE	CLIP-S	RefCLIP-S
Subj01	56.79	36.47	21.85	13.07	21.56	43.20	47.84	14.01	69.14	74.07
Subj02	55.64	36.17	22.01	13.18	20.89	42.55	45.41	13.42	67.63	72.50
Subj05	55.07	35.63	21.70	13.25	20.53	41.83	45.39	12.96	66.94	71.63
Subj07	55.68	35.75	21.60	13.14	20.88	42.32	45.14	13.18	66.94	71.97

Evaluation results of all four subject with complete fMRI data.

Table 2 Hyperparameter tuning

D \ L	2	4	8	16
w/o upe	59.90	58.80	62.16	62.45
2	63.40	67.53	62.60	66.36
4	64.30	69.06	66.90	65.10
6	63.50	68.90	67.70	65.60

Results of model trained with different hyperparameter configurations, evaluated using CLIP scores.

'L', the number of latent channels in projected brain tokens; 'D', the number of layers in transformer architecture; 'upe', the universal perceive encoder (transformer).